The Journal of Antibiotics (2018) 71:939–949
https://doi.org/10.1038/s41429-018-0098-z

JARA Japan Antibiotics Research Association
The Society for Actinomycetes Japan

ARTICLE

Dormant *Mycobacterium tuberculosis* converts isoniazid to the active drug in a Wayne's model of dormancy

Sajith Raghunandanan[1] · Leny Jose[1,2] · Ramakrishnan Ajay Kumar[1]

Received: 21 June 2018 / Accepted: 9 August 2018 / Published online: 5 September 2018

Abstract

Isoniazid (INH) is one among the four first-line drugs used in the treatment of tuberculosis. The bactericidal activity of INH is due to its ability to inhibit mycolic acid synthesis, which is an integral component of the mycobacterial cell wall. Non-replicating *Mycobacterium tuberculosis* (MTB) is phenotypically resistant to INH. The exact mechanism of this resistance is not clear, although the inability of dormant MTB to convert the pro-drug into an active form is thought to be one of the possible reasons. Employing targeted metabolomics approach, we show that dormant MTB can metabolize INH into its active INH-NAD$^+$ adduct form. Further we show that the dormant bacteria have unaltered gene expression levels of *katG* and *inhA* (INH metabolizing enzymes). Transcript levels of drug efflux pump proteins which were low during dormancy did not increase in response to INH treatment. These findings point to an alternative mechanism for INH resistance in dormant MTB, which needs to be further elucidated.

Introduction

Isoniazid (isonicotinic acid hydrazide) is one of the most potent first-line drugs used in the treatment of TB, the others being rifampicin, ethambutol and pyrazinamide. Its clinical activity against MTB was discovered in the early 1950s [1]. INH is bactericidal against MTB in vitro and in vivo including in humans [2]. MTB is most susceptible to INH during its logarithmic phase of growth; the minimum inhibitory concentration (MIC) is 0.2 µg/ml [3]. Interestingly, INH does not have bactericidal activity on non-replicating MTB (one of the reasons why tuberculosis requires prolonged treatment as well as multidrug therapy). INH is a nicotinamide analog, structurally related to ethionamide and pyrazinamide. INH is converted to the active form by MTB catalase-peroxidase (KatG) [4]. The active drug is an isonicotinoyl radical that reacts non-enzymatically with pyridine nucleotide coenzymes, such as NAD, to form an adduct with INH (INH-NAD$^+$) [5, 6]. The INH-NAD$^+$ adduct binds to and inhibits enoyl–acyl carrier protein (ACP) reductase (InhA), resulting in the inhibition of mycolic acid biosynthesis [7–9]. Mycolic acids are high molecular weight, α-alkyl, β-hydroxy fatty acids, which are the major outer cell wall components of mycobacteria [10]. The INH-NAD$^+$ adduct formation has been studied using cell-free assays, and the establishment of the molecular interactions and kinetics of InhA adduct generation have added greater insight into the structure–activity relationship of the drug [11, 12]. Subsequently, binding of INH-NAD$^+$ adduct to recombinant InhA isolated from an *E. coli* strain co-expressing *inhA* and *katG* of MTB was also demonstrated [13].

Molecular mechanism of resistance of MTB to INH is attributed to mutations in the *katG* gene [4, 14]. Mutations reduce the ability of KatG to activate the pro-drug INH, thus leading to drug resistance [15–18]. The most characterized one is the missense mutation $S_{315}T$ (serine $_{315}$ to threonine) [19, 20]. The mutated katG produces a functional catalase-peroxidase with enzymatic activity, but impaired in its ability to form an INH-NAD$^+$ adduct, reducing the INH bactericidal activity [21]. INH resistance also arises due

Electronic supplementary material The online version of this article (https://doi.org/10.1038/s41429-018-0098-z) contains supplementary material, which is available to authorized users.

✉ Ramakrishnan Ajay Kumar
rakumar@rgcb.res.in

[1] Mycobacterium Research Laboratory, Tropical Disease Biology Division, Rajiv Gandhi Centre for Biotechnology, Thycaud P.O, Thiruvananthapuram 695014, India

[2] Department of Dermatology, Indiana University School of Medicine, Indianapolis, IN 46202, USA

to substitutions (T→A; C→A) in *inhA* at the 3′ end of the presumed ribosome binding site located in the region upstream [22]. A single point mutation in *inhA* (Ser $_{94}$ Ala) confers a five-fold increase in resistance to INH, as well as inhibition of mycolic acid biosynthesis [23].

Even though INH is effective in killing actively growing bacilli, it possesses little or no activity against MTB under conditions of nutrient starvation [24] or progressive oxygen depletion in vitro [25]. This resistance mechanism is exhibited by MTB inactivated by a non-replicating persistent state (NRP), which does not involve active cell wall synthesis. To date, it was thought that dormant MTB may not convert INH to the bioactive form, which contributes to resistance [26]. In this study, we report that dormant MTB does actively metabolize INH to its active form. Although none of the proposed mechanisms independently can explain a singular mechanism of INH-resistance in dormant MTB, our study essentially rules out the possibility of non-formation of active INH.

Materials and methods

Bacterial strains and growth conditions

Virulent laboratory strain MTB H37Rv was cultured on Löwenstein–Jensen slants and incubated at 37 °C for 4 to 6 weeks. Broth cultures were prepared by inoculation of one loopful of bacterial colony into Middlebrook 7H9 (BD Difco) medium supplemented with 10% albumin–dextrose–catalase (ADC) and incubated on an orbitary shaker at 130 rpm at 37 °C. All steps involving handling of MTB were carried out in a biosafety level three (BSL3) facility. Validated INH-resistant (INH mono-resistant (Ref no: 567) and multidrug-resistant (MDR) (Ref no: 1565)) strains were a kind gift from the District TB Center, Trivandrum and were cultured by the same protocol. Establishment of dormancy using a modified Wayne's model was performed as described by Gopinath et al. [27].

Drug treatment

To examine the effect of INH on actively growing MTB, a 15-day-old culture was treated with INH (0.2 µg/ml) [28] and was incubated further for 4 days at 130 rpm at 37 °C. Plate count assay was performed on Middlebrook 7H10 agar medium supplemented with 0.5% glycerol, 0.05% Tween 80, and 10% oleate–albumin–dextrose–catalase supplement (Becton Dickinson, Franklin Lakes, NJ, USA). For testing the effect of INH on dormant MTB, INH (0.2 µg/ml) was added to the hypoxic MTB cultures by means of a 25-gauge needle; methylene blue dye did not change color during this process in comparison to the aerobically grown control, indicating that the reduced oxygen tension had not been compromised [26]. Aliquots were withdrawn from each tube on days 1, 2, 3, 7 and 14 after INH treatment and plated onto 7H10 agar plates.

RNA isolation, cDNA synthesis, and quantitative PCR

RNA isolation from dormant/normoxic MTB was carried out using Trizol (Sigma-Aldrich) reagent following the protocol described by Gopinath et al. [27]. Total RNA was resuspended in nuclease-free water and treated with DNase I (Sigma-Aldrich) at 37 °C for 30 min. Complementary DNA (cDNA) was prepared using Reverse Transcriptase Core kit (Eurogentec, Seraing, Belgium) according to the manufacturer's protocol. qPCR reaction was performed using SYBR Green Supermix kit (Bio-Rad). The cycling conditions were set as follows: an initial denaturation at 94 °C for 5 min; 35 cycles of denaturation at 94 °C for 30 s, primer annealing at 59 °C for 30 s, and extension at 72 °C for 40 s, followed by a melt curve analysis. Relative gene expression was performed using $-\Delta\Delta$Ct method, with sigma factor A (*sigA*) as the housekeeping gene control.

Electron microscopy

Twenty milliliters of MTB culture from each condition was centrifuged at 5000 × *g* for 10 min at 25 °C. The pellets were washed thrice in 10 ml ice-cold PBS and centrifuged at 5000 × *g* for 5 min at 25 °C. Pellets were dissolved in 1 ml Dubos Difco broth and vortexed vigorously to disperse the bacterial clumps. Suspensions with an OD of 0.15 were prepared in fresh Dubos broth. Three hundred microliters from each sample was then loaded onto polylysine-coated coverslips that were prepared according to the manufacturer's guidelines (Sigma-Aldrich, St. Louis, MO, USA). Bacteria were allowed to settle for 30 min before gently decanting the medium. One milliliter of 2.5% glutaraldehyde in PBS (pH 7.4) was added to the bacterial film on the coverslip and incubated overnight at 4 °C. A series of dehydration steps was performed for 10 min each in 50, 70, 95 and 100% ethanol and the coverslips were dried at room temperature. Samples were gold-sputtered using JEOL-1200 (Peabody, MA, USA) and imaged using a scanning electron microscope (JEOL-JSM-5600 LV).

Total metabolite isolation from the bacteria

MTB in the states of normoxia and dormancy was centrifuged (5000 × *g*, 10 min, 25 °C). Cell pellets were washed twice in sterile water (10 ml), and 400 mg of the pellet from each condition was then resuspended in 1 ml of sterile PBS. The suspensions were transferred to 2 ml

screw cap microcentrifuge tubes containing glass beads (0.5 mm) and incubated on ice for 5 min. The tubes were then subjected to three, one-minute pulses at 4200 rpm with 1 min interval in a Mini Bead beater (BioSpec Products Inc., Bartlesville, UK). The suspensions were centrifuged for 10 min at 13,000 × *g* (Eppendorf, Hauppauge, NY), and the proteins in the supernatants were precipitated by adding 200 µl of methanol and further incubating at 4 °C for 1 h. The precipitated proteins were removed by centrifuging for 10 min at 4000 × *g* at 25 °C. Supernatant collected was dried using speed vacuum concentrator and resuspended in 50 µl of sterile water.

LC–MS analysis

Liquid chromatography

Analysis was performed using a Waters ACQUITY UPLC™ system (Waters, Milford, MA, USA) coupled to a quadrupole–time-of-flight (Q–TOF) mass spectrometer (SYNAPT-G2, Waters). Both the systems were operated and controlled by MassLynx4.1 SCN781 software (Waters). Metabolite separation was achieved using reverse-phase liquid chromatography employing a C18 (high-strength silica, 2.1 × 100 mm, 1.8 µm; Waters) column. Briefly, a 7.5 µl aliquot of each sample was injected into the column maintained at 40 °C. For each sample, the run time was 20 min with a flow rate of 400 µl/min. The mobile phase consisted of aqueous (A) and organic (B) solvent components, where A was 0.1% formic acid in ultrapure water and B was 0.1% formic acid in acetonitrile. The gradient was 0 min, 1% B; 2 min, 10% B; 6 min, 30% B; 8 min, 50% B; 12 min, 75% B; 15 min, 99% B; and 20 min, 1% B. Each sample was injected in triplicate with blank injections between each sample.

Mass spectrometry

The SYNAPT® G2 High Definition MS™ System mass spectrometer (Waters) was operated in positive and negative resolution mode with electrospray ionization (ES^+) source over a mass range of 50–1500 Da. Each spectrum was acquired for 0.25 s with an interscan delay of 0.024 s. Ion source and desolvation gas (nitrogen) temperatures were kept at 130 °C and 450 °C, respectively. The cone and desolvation gas flow rates were 80 L/h and 600 L/h, respectively. Capillary voltage was set at 3.0 kV, and sampling cone voltage was set at 30 kV. Lock mass acquisition was performed every 30 s by leucine–enkephalin (556.2771 $[M+H]^+$) for accurate on-line mass calibration. Data acquisition was carried out in centroid mode and processed using MassLynx software.

Data processing

MassLynx4.1 SCN781 (Waters) was used for data acquisition and collection. Markerlynx XS software (Waters) was employed for peak/feature picking and raw data deconvolution, noise filtering, peak detection, isotope peak removal, alignment of retention time and mass, and optional peak/feature normalization. Method parameters for Markerlynx processing were as follows: peak width at 5% height - 1 S; marker intensity threshold-10 counts; mass window - 0.05 Da, and retention time window - 0.2 min. Chemical formula substitution and naming of compounds were performed using MassLynx4.1 SCN781 within 5 ppm range and further verified using ChemSpider chemical structure database. The masses were further validated using MassTRIX available at http://masstrix3.helmholtz-muenchen.de/masstrix3/start.html.

Results

Dormant MTB is resistant to INH

To test INH resistance in dormant MTB, we performed a series of plate count assays after treating dormant MTB and actively growing bacilli (control) with lethal concentration of INH (0.2 µg/ml). Upon INH treatment, actively growing MTB showed significant reduction in bacterial count with 100% killing 16 days after drug treatment (Fig. 1a). Viable count of dormant MTB was not affected by treatment with INH even after 35 days and the cell numbers remained relatively constant throughout the treatment time points, indicating that bacteria are indeed dormant and resistant to INH (Fig. 1b). Effect of INH on the bacterial morphology was analyzed using scanning electron microscopy. Log-phase MTB treated with INH showed characteristic morphological changes (Fig. 1c, d). Interestingly, no such morphological changes were observed in dormant MTB treated with the same concentration of INH (Fig. 1e, f). However, dormant MTB appeared fragile due to cavitation and thinning of the cell wall (Fig. 1c, e).

Expression of *katG* and *inhA* is comparable in INH-treated and untreated dormant MTB

To test if *katG* expression played a role in INH resistance in dormant MTB, we compared the expression of *katG* during normoxia and dormancy by qPCR. Interestingly, *katG* expression was found to be similar in dormant MTB and log-phase bacteria (Fig. 2a). Reanalysis of KatG protein levels in NRP-1 and NRP-2 stages of

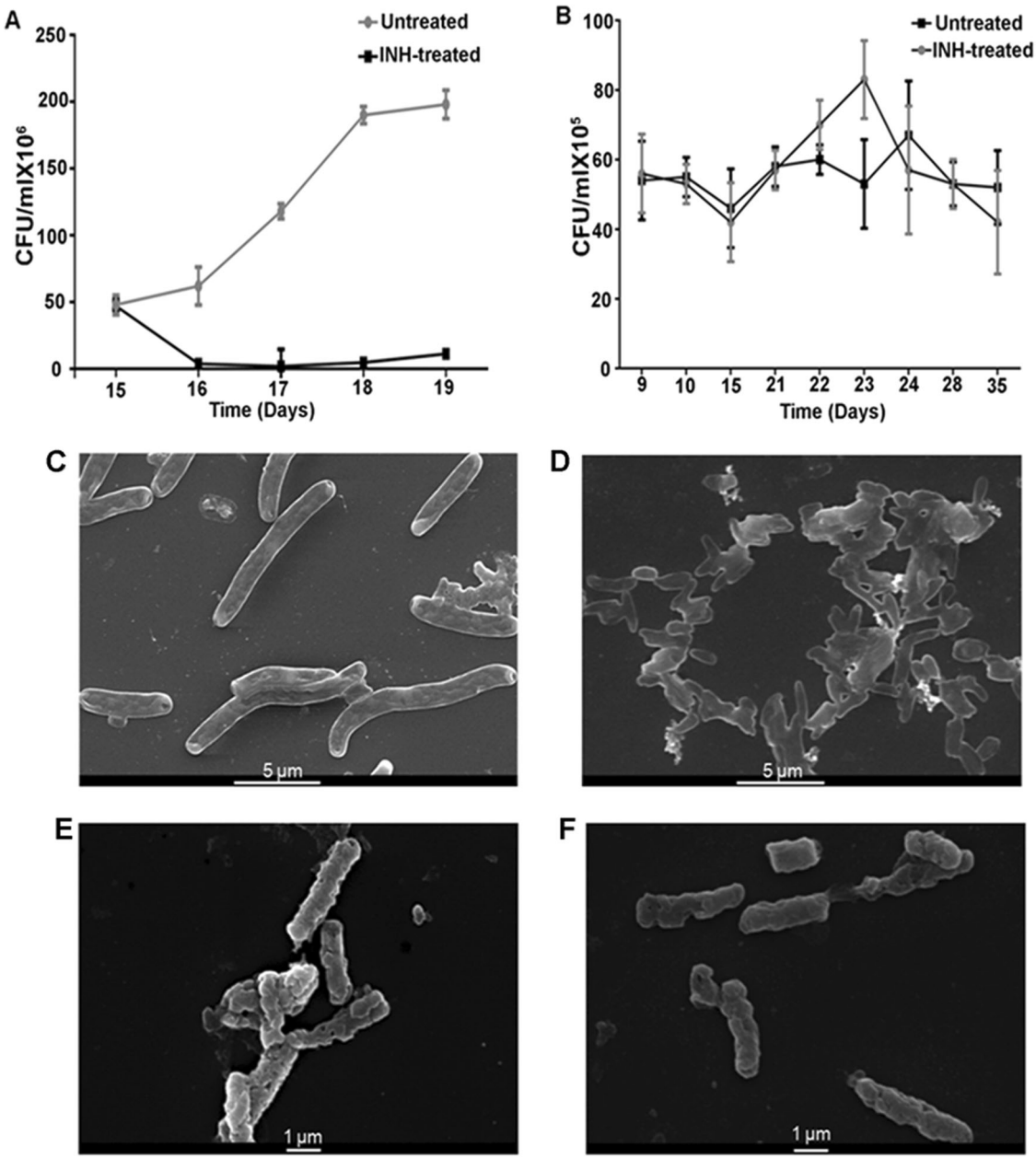

Fig. 1 Effect of INH (0.20 µg/ml) on the viability of log-phase (Control) and dormant MTB. **a** 15-day-old MTB grown in Middlebrook 7H9 medium was treated with 0.20 µg/ml of INH, and viable cells were counted (CFU/ml) on days 16, 17, 18 and 19. **b** 21-day-old dormant MTB was treated with the same concentration of INH, grown under hypoxic condition, and viable cells were counted on days 22, 23, 24, 28 and 35. In both experiments, untreated MTB at same time points was used as control. Results from a representative sample of two biological replicates are shown. The error bars indicate standard deviations of the mean colony counts. Morphology of log-phase and dormant MTB upon treatment with INH. Scanning electron microscopic (SEM) images showing **c** log-phase MTB, **d** INH-treated log-phase cells, **e** dormant MTB, and **f** INH-treated dormant MTB. Magnification - 5000× for (**c**) and (**d**), and 10,000× for (**e**) and (**f**), respectively

dormancy from our previous proteomics study also showed similar results (Fig. 2b) [27]. *katG* expression remained comparable in dormant and actively growing MTB treated with INH, compared with untreated bacteria (Fig. 2c). Next we examined the expression levels of *inhA* under the same conditions. Similar to *katG*, expression of *inhA* also remained similar in both dormant and actively growing MTB (Fig. 2d). From the analysis of the proteomics data from our previous studies, we found that InhA levels were comparable in dormant and actively growing MTB (Fig. 2e) [27]. *inhA* expression remained unchanged in dormant and actively growing MTB treated with INH, compared with untreated controls (Fig. 2f).

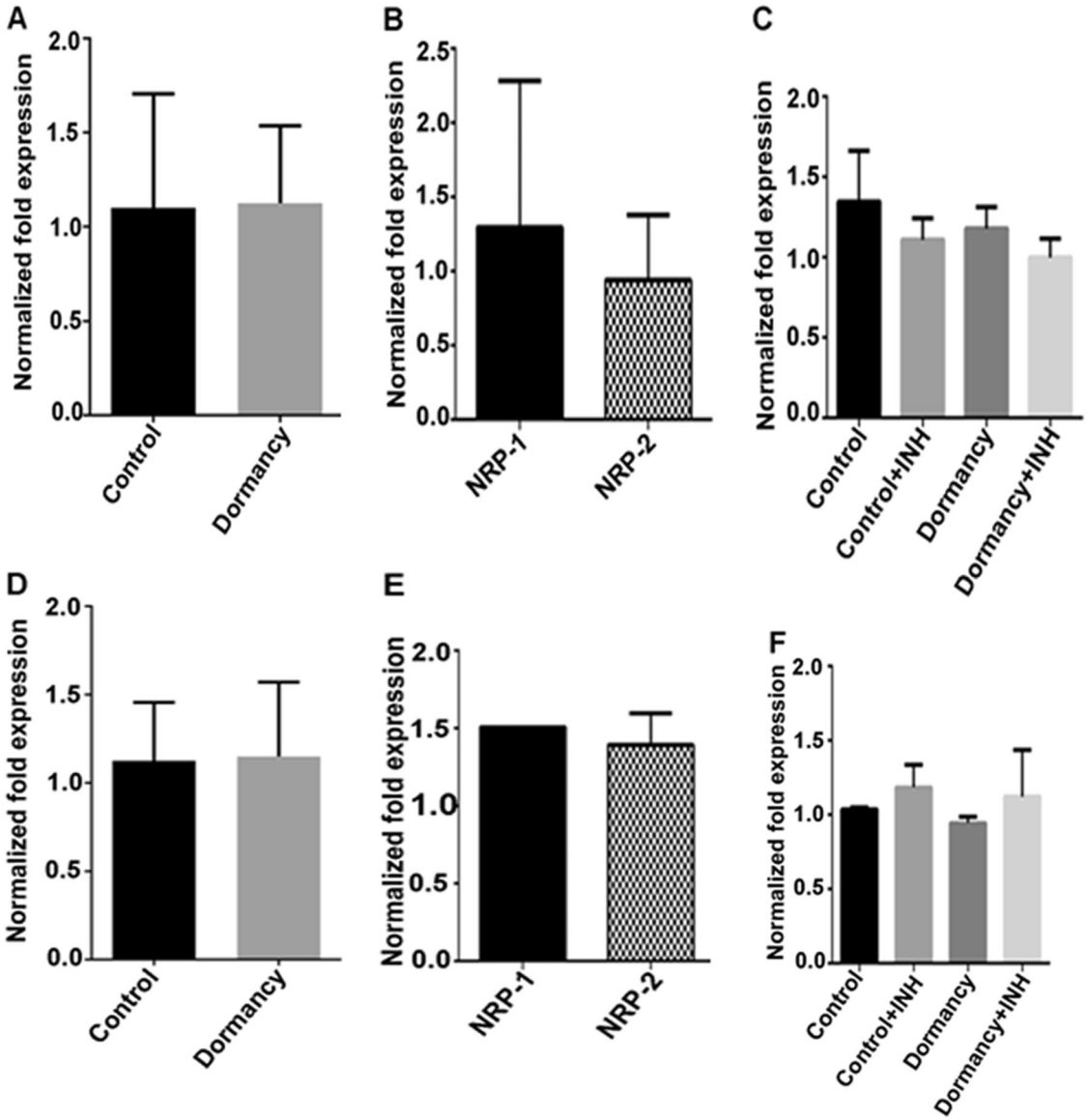

Fig. 2 *katG* and *inhA* expression in log-phase and dormant MTB. **a** k*atG* expression in log-phase and dormant MTB. **b** quantitative proteomic analysis of KatG during non-replicating persistence stage-1 (NRP-1) and non-replicating persistence stage-2 (NRP-2) [27]. **c** *katG* expression during log-phase and dormancy in INH-treated and untreated MTB. **d** *inhA* expression in log-phase and dormant MTB. **e** quantitative proteomic analysis of InhA during non-replicating persistence stage-1 (NRP-1) and non-replicating persistence stage-2 (NRP-2) [27]. **f** *inhA* expression during log-phase and dormancy in INH-treated and untreated MTB. The results are expressed as relative fold expression after normalizing with *sigA*, the endogenous control. Results are represented as mean of two biological replicates ± standard deviation

Drug efflux pumps in MTB are downregulated during dormancy, but do not respond to INH treatment

Since *katG* and *inhA* expression remained unaltered during dormancy, we wondered if drug efflux pumps were used by the dormant bacteria to expel INH from the cell. We selected five of the best-known MTB efflux pump proteins for analysis – IniA, PstB, BacA, MmR, and EfpA [29–33]. Surprisingly, the mRNA levels of all these efflux pump proteins were significantly down in dormant MTB when compared to actively growing bacteria (Fig. 3a). Interestingly, when dormant MTB was treated with INH, it did not display an upregulation of any of the genes coding for these efflux pump proteins (Fig. 3c), whereas *iniA*, *pstB,* and *efpA* were found to be upregulated significantly in normoxially grown INH-treated MTB (Fig. 3b).

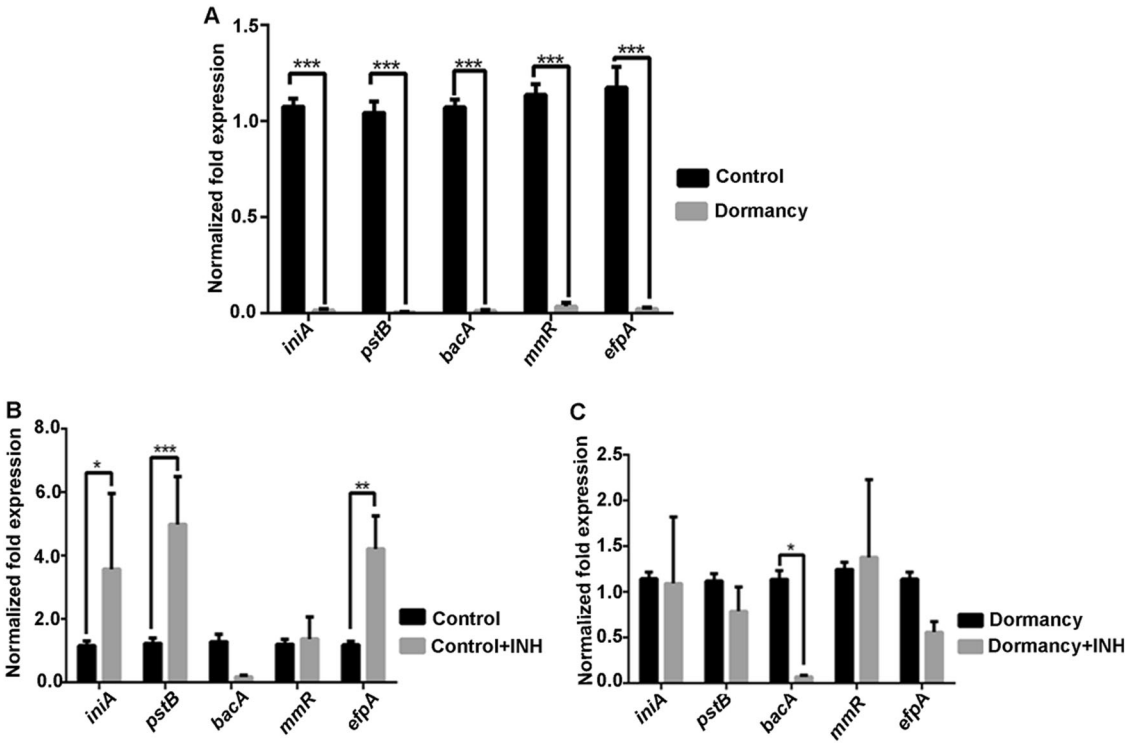

Fig. 3 **a** Expression profile of efflux pump protein genes - *iniA*, *pstB*, *bacA*, *mmR*, and *efpA* during normoxia (control) and dormancy. **b** Expression profile of the same genes in log-phase MTB and in MTB treated with INH. **c** Expression of the same genes in dormant MTB and INH-treated dormant MTB. The results are expressed as relative fold expression after normalizing with *sigA*, the endogenous control. Results are represented as the mean of two biological replicates ± standard deviation (Student's *t*-test). $***P \leq 0.001$, $**P \leq 0.01$ and $*P \leq 0.1$

Meta-analysis of INH-treated MTB

Identification of INH and INH-NAD$^+$ adduct in bacterial metabolome

To test if INH is metabolized to active INH-NAD$^+$ adduct by dormant MTB, we isolated total metabolites from dormant and actively dividing MTB treated with INH for 24 and 48 h. INH (Sigma-Aldrich) was used as mass standard for LC–MS analysis. In a 20 min run using water:acetonitrile gradient, we observed a peak at 0.84 s which corresponded to INH with a molecular mass of 138.067 Da (Fig. 4a, e), and this mass was absent in metabolites isolated from untreated MTB (Fig. 4d, h). Similarly, we were able to identify small amounts of the pro-drug (INH) from actively dividing (Fig. 4b, c, f, g) and dormant (Fig. 5b, c, f, g) MTB (24 and 48 h post treatment) at the same retention time. We were able to identify INH (Fig. S1A, C, B & D) even in the clinical isolates (INH mono-resistant and MDR) after 48 h of INH treatment. Interestingly, there was a significant reduction in the quantities of INH at 24-48 h in actively growing MTB.

Active form of INH (INH-NAD$^+$ adduct) has a molecular mass of 769.34 Da [34]. From our meta-analysis, we were able to identify this mass from actively dividing MTB treated with INH (24 and 48 h). In a 20 min metabolite run, a peak which corresponded to 769.34 Da was observed at 10.03 min from actively dividing MTB (Fig. 6a, b, e, f). This mass was absent in metabolites from untreated MTB. Quite interestingly, INH-NAD$^+$ adduct was absent among the metabolites isolated from INH-resistant MTB strains treated with INH (Fig. S2A, B, C &D). This was expected because both the strains (INH mono-resistant and MDR) have $S_{315}T$ mutation in their KatG, as a result of which they could not convert the pro-drug into the active form. Remarkably, we observed that dormant MTB could convert the pro-drug to INH-NAD$^+$ adduct at 24 and 48 h after INH treatment (Fig. 7a, b, d, e). The efficiency of conversion was similar to that by actively growing the bacteria as evidenced by comparable peak heights (Figs. 6e, f and 7d, e).

Discussion

Two distinct mechanisms contribute to resistance against INH in MTB, the first and most studied being chromosomal mutations in INH response genes. The second mechanism

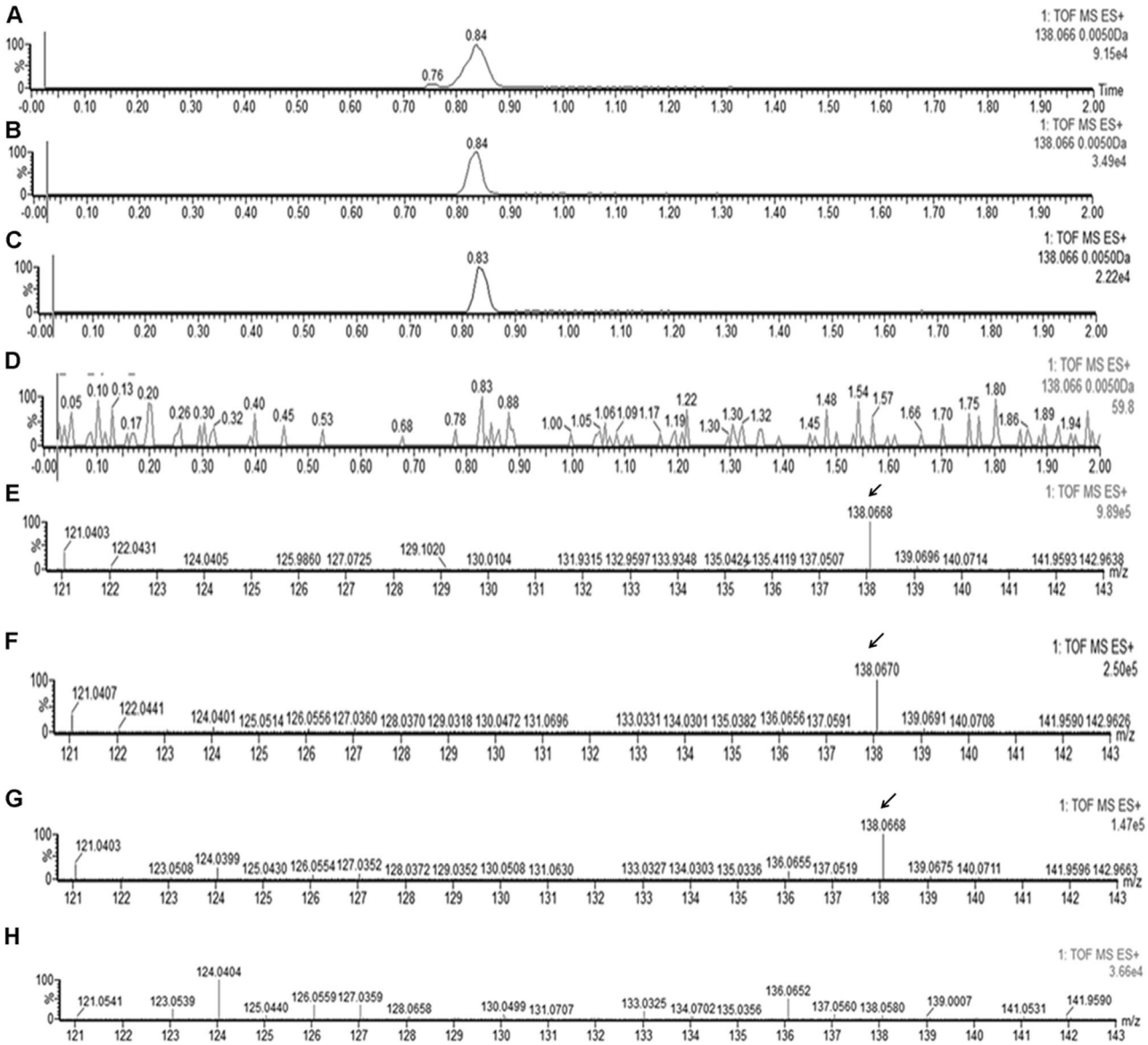

Fig. 4 Meta-analysis to identify INH in log-phase MTB. **a** Extracted ion chromatograms (EIC) of INH (500 ng/µl) dissolved in water (standard). EIC of INH from total metabolites identified from log-phase MTB after (**b**) 24 and (**c**) 48 h of INH treatment. **d** EIC of metabolites isolated from untreated MTB culture. MS spectra (showing m/z) of the EIC. **e** INH standard. MTB after 24 (**f**) and 48 h (**g**) of INH treatment. **h** Untreated MTB culture. m/z of INH is marked by arrows in all panels. In all the panels, intensities of expected mass are given at the top right of the mass spectra

is the acquisition of growth phase-dependent phenotypic resistance to INH. Alternatively called INH tolerance, this occurs during the stationary phase of growth, hypoxia, or dormancy and is one of the reasons for the need for prolonged chemotherapy due to emergence of a subpopulation of bacteria called persistors. Conditions of progressive hypoxia or nutrient starvation can induce INH resistance in MTB [26]. Transcriptional profiling of MTB during these conditions revealed that lack of INH response genes correlated with INH resistance [26]. A similar study that used Wayne's model of dormancy to probe the sensitivity of bacilli to INH by transcriptional profiling reports that INH treatment failed to elicit a transcriptional response from non-replicating bacteria (NRP-2) [35]. Our analysis of *katG* and *inhA* transcripts also confirmed that the expression levels of these genes are unaltered during dormancy and INH treatment. Another hypothesis is that the cell wall of dormant MTB prevents entry of the pro-drug into the intracellular compartment. There is compelling evidence that there is a metabolic shift from lipid biosynthesis to lipid degradation in the cell wall during dormancy [27]. It is evident from the photomicrographs that dormant MTB cells showed significant cavitation and thinning of the cell wall that lent them a fragile appearance. The cells also showed a

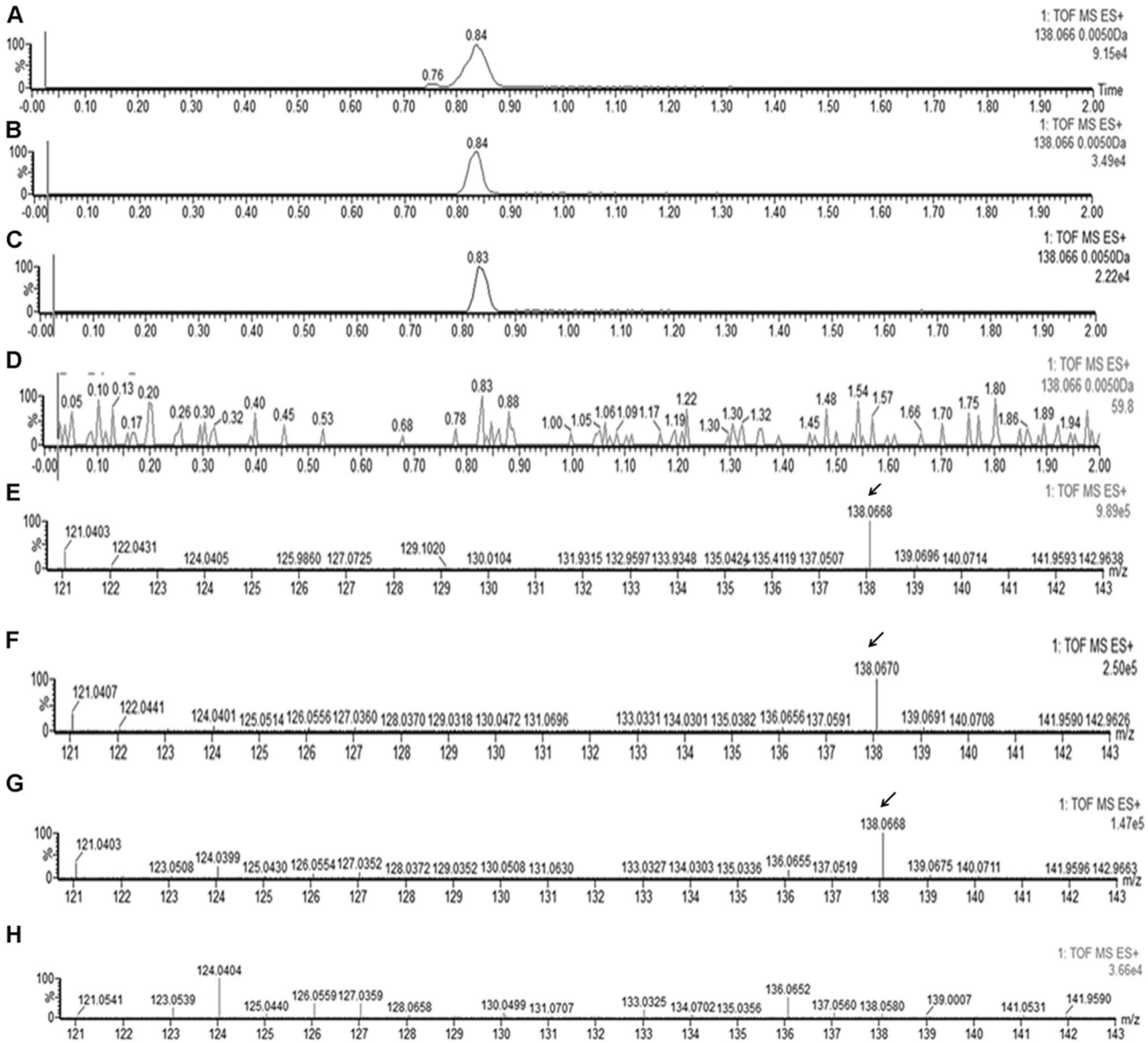

Fig. 5 Meta-analysis to identify INH from dormant MTB. **a** Extracted ion chromatograms (EIC) of INH (500 ng/µl) dissolved in water (standard). EIC of INH from total metabolites identified from dormant MTB after (**b**) 24 and (**c**) 48 h of INH treatment. **d** EIC of metabolites isolated from untreated MTB culture. MS spectra (showing m/z) of the EIC. **e** INH standard; dormant MTB after 24 (**f**) and 48 h (**g**) of INH treatment. **h** Untreated dormant MTB metabolites. m/z of INH is marked by arrows in all panels. In all the panels, intensities of expected mass is given at the top right of the mass spectra

decrease in size (1-2 µm) when compared to the log-phase MTB (8-10 µm). However, treatment of dormant MTB with INH did not cause any alterations in cell morphology compared to the untreated dormant bacteria. INH penetrates host cells readily; its antimycobacterial activity was found to be equal against intracellular and extracellular MTB in vitro [36]. Detection of INH and its metabolic byproducts from INH-treated MTB has been recognized as a challenging task requiring high sensitivity and precision metabolomics approaches [37]. Most of the chemical modifications that INH undergoes inside the bacilli including formation of INH-NAD$^+$ adduct have been demonstrated only through cell-free assays [38]. The first attempt in this direction used a LC/MS-based metabolomics approach to detect INH or any of its byproducts in the urine collected from TB patients undergoing drug treatment. Mahapatra et al. (2015) were unable to detect INH-NAD$^+$ adducts from the urine samples of INH-treated TB patients, although they detected 4-isonicotinoyl nicotinamide (4-INN), which they propose to result from the hydrolysis of the INH-NAD$^+$ adduct. Host enzymes like lactoperoxidases are also capable of metabolizing INH, and the same authors found that mice which were not infected with MTB, but treated with INH, also secreted 4-INN. 4-INN was found in the urine of

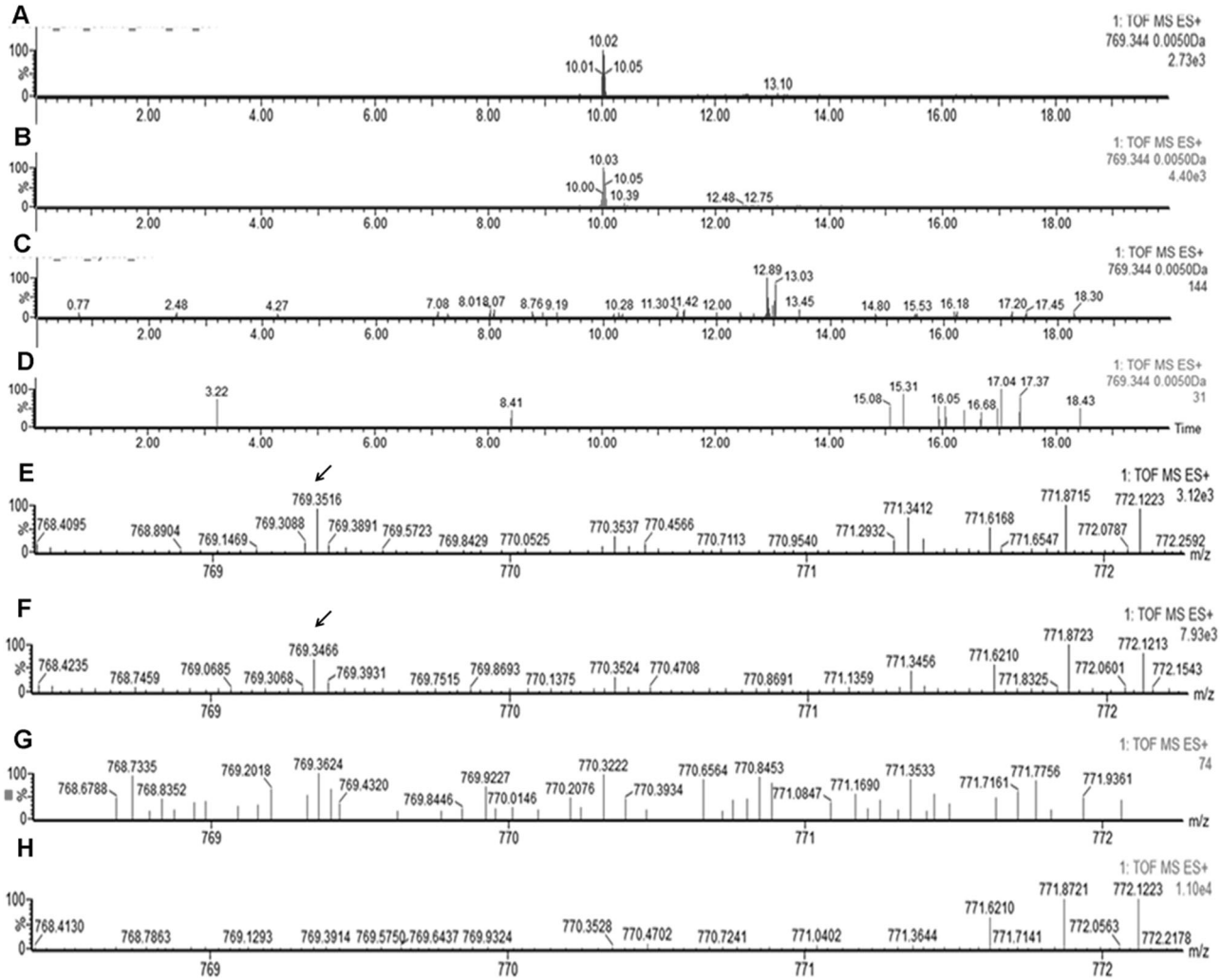

Fig. 6 Meta-analysis to identify INH-NAD$^+$ adduct from log-phase MTB. Extracted ion chromatograms (EIC) of INH-NAD$^+$ adduct (769.34 Da), with a retention time of 10 min identified from metabolites of log-phase MTB treated with INH after 24 (**a**) and 48 h (**b**) of INH treatment. However, this mass is absent in standard (**c**), and untreated MTB metabolites (**d**) at same retention time. MS spectra (showing m/z) of the EIC of the peak eluted at the 10th min of the run from log-phase MTB after 24 (**e**) and 48 h (**f**) of INH treatment. Active INH-NAD$^+$ adduct is absent in standard (**g**), and untreated MTB metabolites (**h**). m/z of INH-NAD$^+$ adduct is marked by arrows in all panels. In all the panels, the intensities of expected mass are given at the top right of the mass spectra

culture-negative TB patients also [34]. As this conversion is possibly mediated by host enzymes, the utility of 4-INN as a marker for INH activation in TB infection is limited [39]. In another study which analyzed the plasma metabolome of adult pulmonary TB patients treated with first-line drugs detected the m/z for INH at low intensity, but did not detect any INH metabolites other than acetylhydrazine (m/z 97.0389) and isoniazid pyruvate (m/z 208.0682) [40]. In our in vitro model of dormancy, which is based on the Wayne's model of progressive hypoxia, we show that INH penetrates dormant bacilli and can be readily detected in the metabolome. Also for the first time, using targeted metabolomics approach, we demonstrate that dormant MTB can actively metabolize INH to active INH-NAD$^+$ adduct. Our observations contradict the current hypothesis that INH resistance in dormant MTB is due to the inability of dormant MTB to convert INH to its active metabolite. We propose that the phenotypic resistance of dormant bacteria could be attributed to hitherto unknown factors that target biochemical steps downstream of INH adduct formation. Further investigation is needed to tease out the mechanism of growth phase-induced INH tolerance in MTB.

Acknowledgements This study has been funded by the Department of Biotechnology, Government of India [BT/PR5361/MED/29/507/2012 (RAK)]. SR is grateful for the INSPIRE fellowship from the Department of Science and Technology, Government of India. We thank the Mass Spectrometry and Proteomic Core Facility of RGCB for mass spectrometry analysis.

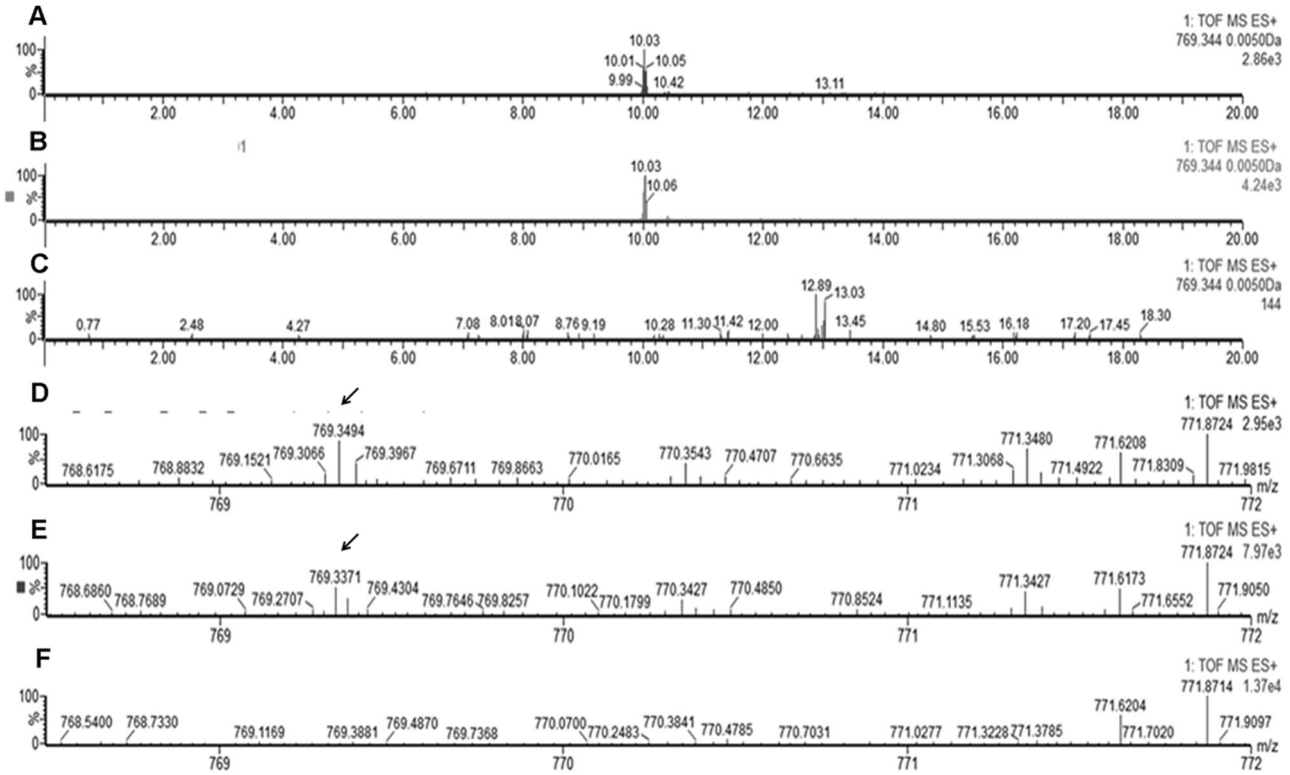

Fig. 7 Meta-analysis to identify INH-NAD$^+$ adduct from dormant MTB. Extracted ion chromatograms (EIC) of INH-NAD$^+$ adduct (769.34 Da), with a retention time of 10 min identified from metabolites of dormant MTB treated with INH after 24 (**a**) and 48 h (**b**) of INH treatment. However, this mass is absent in untreated dormant MTB metabolites at the same retention time (**c**). MS spectra (showing m/z) of the EIC of the peak eluted at the 10th min of the run (**e**) from dormant MTB after 24 (**d**) and 48 h (**e**) of INH treatment. Active INH-NAD$^+$ adduct is absent in untreated dormant MTB metabolites (**f**). m/z of INH-NAD$^+$ adduct is marked by arrows in all panels. In all the panels, the intensities of expected mass are given at the top right of the mass spectra

Author contributions Conceptualization, RAK and SR; methodology, SR, LJ and RAK; investigation, SR and RAK; formal analysis, SR and RAK; writing, SR, LJ and RAK; and resources, RAK.

Compliance with ethical standards

Conflict of interest The authors declare that they have no conflict of interest.

References

1. Robitzek EH, Selikoff IJ. Hydrazine derivatives of isonicotinic acid (Rimifon, Marsilid) in the treatment oi active progressive caseous-pneumonic tuberculosis. A preliminary report. Am Rev Tuberc Pulm Dis. 1952;65:402–28.
2. Jindani A, Aber V, Edwards E, Mitchison D. The early bactericidal activity of drugs in patients with pulmonary tuberculosis. Am Rev Respir Dis. 1980;121:939–49.
3. Reller LB, Weinstein MP, Woods GL. Susceptibility testing for mycobacteria. Clin Infect Dis. 2000;31:1209–15.
4. Zhang Y, Heym B, Allen B, Young D, Cole S. The catalase-peroxidase gene and isoniazid resistance of *Mycobacterium tuberculosis*. Nature. 1992;358:591.
5. Johnsson K, Schultz PG. Mechanistic studies of the oxidation of isoniazid by the catalase peroxidase from *Mycobacterium tuberculosis*. J Am Chem Soc. 1994;116:7425–6.
6. Lei B, Wei C-J, Tu S-C. Action mechanism of antitubercular isoniazid activation by *Mycobacterium tuberculosis* KatG, isolation, and characterization of InhA inhibitor. J Biol Chem. 2000;275:2520–6.
7. Banerjee A, Dubnau E, Quemard A, Balasubramanian V, Um KS, Wilson T, et al. inhA, a gene encoding a target for isoniazid and ethionamide in *Mycobacterium tuberculosis*. Science. 1994;263:227–30.
8. Takayama K, Wang L, David HL. Effect of isoniazid on the in vivo mycolic acid synthesis, cell growth, and viability of *Mycobacterium tuberculosis*. Antimicrob Agents Chemother. 1972;2:29–35.
9. Winder F, Collins P. Inhibition by isoniazid of synthesis of mycolic acids in *Mycobacterium tuberculosis*. Microbiology. 1970;63:41–8.
10. Brennan PJ, Nikaido H. The envelope of mycobacteria. Annu Rev Biochem. 1995;64:29–63.
11. Rawat R, Whitty A, Tonge PJ. The isoniazid-NAD adduct is a slow, tight-binding inhibitor of InhA, the *Mycobacterium tuberculosis* enoyl reductase: adduct affinity and drug resistance. Proc Natl Acad Sci. 2003;100:13881–6.
12. Rozwarski DA, Grant GA, Barton DH, Jacobs WR, Sacchettini JC. Modification of the NADH of the isoniazid target (InhA) from *Mycobacterium tuberculosis*. Science. 1998;279:98–102.
13. Wang F, Jain P, Gulten G, Liu Z, Feng Y, Ganesula K, et al. *Mycobacterium tuberculosis* dihydrofolate reductase is not a target relevant to the antitubercular activity of isoniazid. Antimicrobial agents and chemotherapy. 2010;54:3776–82.

14. Zhang Y, Garbe T, Young D. Transformation with katG restores isoniazid-sensitivity in *Mycobacterium tuberculosis* isolates resistant to a range of drug concentrations. Mol Microbiol. 1993;8:521–4.
15. Ferrazoli L, Palaci M, da Silva Telles MA, Ueki SY, Kritski A, Marques LRM, et al. Catalase expression, katG, and MIC of isoniazid for *Mycobacterium tuberculosis* isolates from Sao Paulo, Brazil. Journal of Infectious Diseases. 1995;171:237–40.
16. Kapur V, Li L-L, Hamrick MR, Plikaytis BB, Shinnick TM, Telenti A, et al. Rapid Mycobacterium species assignment and unambiguous identification of mutations associated with antimicrobial resistance in *Mycobacterium tuberculosis* by automated DNA sequencing. Archives of pathology & laboratory medicine. 1995;119:131–8.
17. Marttila HJ, Soini H, Eerola E, Vyshnevskaya E, Vyshnevskiy BI, Otten TF, et al. A Ser315Thr substitution in KatG is predominant in genetically heterogeneous multidrug-resistant *Mycobacterium tuberculosis* isolates originating from the St. Petersburg area in Russia. Antimicrobial agents and chemotherapy. 1998;42:2443–5.
18. Telenti A. Genetics of drug resistant tuberculosis. Thorax. 1998;53:793–7.
19. Gagneux S, Burgos MV, DeRiemer K, Enciso A, Muñoz S, Hopewell PC, et al. Impact of bacterial genetics on the transmission of isoniazid-resistant *Mycobacterium tuberculosis*. PLoS pathogens. 2006;2:e61.
20. Yu S, Girotto S, Lee C, Magliozzo RS. Reduced affinity for isoniazid in the S315T mutant of *Mycobacterium tuberculosis* KatG is a key factor in antibiotic resistance. J Biol Chem. 2003;278:14769–75.
21. Pym AS, Saint-Joanis B, Cole ST. Effect of katG mutations on the virulence of *Mycobacterium tuberculosis* and the implication for transmission in humans. Infect Immun. 2002;70:4955–60.
22. Kiepiela P, Bishop K, Smith A, Roux L, York D. Genomic mutations in the katG, inhA and aphC genes are useful for the prediction of isoniazid resistance in *Mycobacterium tuberculosis* isolates from Kwazulu Natal, South Africa. Tuber Lung Dis. 2000;80:47–56.
23. Vilchèze C, Wang F, Arai M, Hazbón MH, Colangeli R, Kremer L, et al. Transfer of a point mutation in *Mycobacterium tuberculosis* inhA resolves the target of isoniazid. Nature medicine. 2006; 12:1027.
24. Betts JC, Lukey PT, Robb LC, McAdam RA, Duncan K. Evaluation of a nutrient starvation model of *Mycobacterium tuberculosis* persistence by gene and protein expression profiling. Mol Microbiol. 2002;43:717–31.
25. Wayne LG, Hayes LG. An in vitro model for sequential study of shiftdown of *Mycobacterium tuberculosis* through two stages of nonreplicating persistence. Infect Immun. 1996;64:2062–9.
26. Karakousis PC, Williams EP, Bishai WR. Altered expression of isoniazid-regulated genes in drug-treated dormant *Mycobacterium tuberculosis*. J Antimicrob Chemother. 2007;61:323–31.
27. Gopinath V, Raghunandanan S, Gomez RL, Jose L, Surendran A, Ramachandran R, et al. Profiling the proteome of *Mycobacterium tuberculosis* during dormancy and reactivation. Molecular & Cellular Proteomics. 2015;14:2160–76.
28. Pontino M, Di BG, Fernandez C, Imperiale B, Bodon A, Morcillo N. Evaluation of a colorimetric micromethod for determining the minimal inhibitory concentration of antibiotics against *Mycobacterium tuberculosis*. Rev Argent Microbiol. 2006;38: 145–51.
29. Louw G, Warren R, van Pittius NG, McEvoy C, Van Helden P, Victor T. A balancing act: efflux/influx in mycobacterial drug resistance. Antimicrob Agents Chemother. 2009;53:3181–9.
30. Narang A, Giri A, Gupta S, Garima K, Bose M, Varma-Basil M. Contribution of putative efflux pump genes to isoniazid resistance in clinical isolates of *Mycobacterium tuberculosis*. Int J mycobacteriology. 2017;6:177.
31. da Silva PEA, Von Groll A, Martin A, Palomino JC. Efflux as a mechanism for drug resistance in *Mycobacterium tuberculosis*. FEMS Immunol & Med Microbiol. 2011;63:1–9.
32. Rodrigues L, Villellas C, Bailo R, Viveiros M, Aínsa JA. Role of the Mmr efflux pump in drug resistance in *Mycobacterium tuberculosis*. Antimicrob Agents Chemother. 2013;57:751–7.
33. Li G, Zhang J, Guo Q, Jiang Y, Wei J, Zhao L-l, et al. Efflux pump gene expression in multidrug-resistant *Mycobacterium tuberculosis* clinical isolates. PLoS ONE. 2015;10: e0119013.
34. Mahapatra S, Woolhiser LK, Lenaerts AJ, Johnson JL, Eisenach KD, Joloba ML, et al. A novel metabolite of antituberculosis therapy demonstrates host activation of isoniazid and formation of the isoniazid-NAD+ adduct. Antimicrobial agents and chemotherapy. 2012;56:28–35.
35. Tudó G, Laing K, Mitchison DA, Butcher PD, Waddell SJ. Examining the basis of isoniazid tolerance in nonreplicating *Mycobacterium tuberculosis* using transcriptional profiling. Future Med Chem. 2010;2:1371–83.
36. Suter E. Multiplication of tubercle bacilli within phagocytes cultivated in vitro, and effect of streptomycin and isonicotinic acid hydrazide. Am Rev Tuberc Pulm Dis. 1952;65:775–6.
37. Loots DT. An altered *Mycobacterium tuberculosis* Metabolome Induced by katG mutations resulting in isoniazid resistance. Antimicrob Agents Chemother. 2014;58:2144–9.
38. Timmins GS, Deretic V. Mechanisms of action of isoniazid. Mol Microbiol. 2006;62:1220–7.
39. Choi SW, Maiga M, Maiga MC, Atudorei V, Sharp ZD, Bishai WR, et al. Rapid in vivo detection of isoniazid-sensitive *Mycobacterium tuberculosis* by breath test. Nature Communications. 2014;5:4989.
40. Frediani JK, Jones DP, Tukvadze N, Uppal K, Sanikidze E, Kipiani M, et al. Plasma Metabolomics in Human Pulmonary Tuberculosis Disease: A Pilot Study. PLoS ONE. 2014;9: e108854.